This article has been accepted for publication in a future issue of this journal, but has not been fully edited. Content may change prior to final publication. Citation information: DOI 10.1109/ACCESS.2020.3020892, IEEE Access

IEEE Access
Multidisciplinary ⋮ Rapid Review ⋮ Open Access Journal

Date of publication xxxx 00, 0000, date of current version xxxx 00, 0000.

Digital Object Identifier 10.1109/ACCESS.2020.Doi Number

Aided Image Acquisition System for Aerobics Training Based on Motion Recognition Technology

Haiying Guo[1,2,a], Hui Liu[1,b], Xiaoming Liu[3,c*]
[1]College of Physical Education, Jinzhong University, Jinzhong 030600, Shanxi, China
[2]Kyungsung University, Busan 48434, Korea
[3]Shaoxing University, Shaoxing 312000, Zhejiang, China

[a]Email:ghy_791204@126.com
[b]Email:lh_780722@126.com
[c]Email:xliu7879@163.com

*Corresponding Author Xiaoming Liu (Email:xliu7879@163.com)

This work was supported by 2017 Shanxi Provincial Soft Science Research Project: Research on Establishment of Young Students' Physical Health Monitoring and Management System Based on Internet Plus in Shanxi Province (project number: 2017041042-4); 2019 Colleges and Universities Teaching Reform Innovation Project of Shanxi Province: Research on Sports Compound Talent Training Model Based on Internet Plus Health (Project Number: J2019187)

Abstract The image acquisition system is the main part of acquiring image information, and its performance largely determines the accuracy and difficulty of subsequent planning. The main purpose of this article is to design an image acquisition system for aerobics training based on motion recognition technology. This article mainly introduces the teaching experiments based on the design of aerobics courses. Through the empirical investigation and analysis of the impact of relevant experimental data on aviation training courses, attempts to establish the connection between aerobics social adaptability and various dimensions The cultivation of student's social adaptability. In this paper, the GMM algorithm is mainly used to distinguish the rest time when the action occurs, and the subsequent rest period is used as the basis for segmenting multiple events in the action sequence. Finally, the characteristics of the action coding mapping of each event are derived, and the support vector machine is used to complete the energy recognition process of the existence of a single energy. The experimental results of this paper show that the designed embedded image acquisition system has high integration and stability, the acquired image resolution is 640x480, and the wireless transmission rate is 5MbPs, which has wide application prospects.

Keywords: Aerobics Training, Image Acquisition System, Motion Recognition Technology, Wireless Transmission Technology, GMM Algorithm

I. INTRODUCTION

A. BACKGROUND AND SIGNIFICANCE

For now, with the development of Internet technology, the network and communications industry has developed rapidly, video image acquisition technology has also made unprecedented development and progress, and the research power of image acquisition technology has also been greatly strengthened. Image acquisition system with image acquisition, storage, transmission, real-time display functions, high cost performance, flexible installation site, and high adaptability to the environment. Most of the systems designed based on the PC platform are more traditional image acquisition and transmission systems, and their transmission mode is the wired transmission mode. Using a wireless transmission system, the collected live images will be transmitted wirelessly, reducing the workload and saving the application cost of the system. In addition, the system is more integrated, the working performance is more stable, and the system is lost.

In recent years, sports knowledge has made a lot of progress, but it also faces many issues. There are many ways to solve various problems encountered in identifying traffic flow. In order to recognize different actions, it is useful to recognize the actions before segmenting the video and identifying the actions. This method does not depend on the action restrictions in the video, and divides the entire video into a whole. In other methods, sliding windows are used to divide the entire video sequence into multiple overlays. Other methods can simulate transitions between actions.

B. RELATED WORK

Behrens M proposed an improved aerobic exercise program designed to improve the neuromuscular and musculoskeletal function of the legs. And conducted a randomized controlled

This work is licensed under a Creative Commons Attribution 4.0 License. For more information, see https://creativecommons.org/licenses/by/4.0/.

This article has been accepted for publication in a future issue of this journal, but has not been fully edited. Content may change prior to final publication. Citation information: DOI 10.1109/ACCESS.2020.3020892, IEEE Access

trial study to evaluate the feasibility of conducting a large-scale study. Here, he reports on the effects of training on flexion neuromuscular function. However, since the subjects of the experiment are the elderly, all the conclusions drawn are not very accurate [1]. Gupta PS proposes an imaging system design method and uses a simplified image sensor pixel design in the system so that compressed sensing (CS) technology can be easily implemented at the sensor level. This not only saves the original data rate, but also reduces the number of transistors per pixel, so it can save a lot of energy and reduce the pixel size. However, the design of this system is too complicated and not suitable for some high-pixel images [2]. Zhang J proposed an adaptive method to enhance the recognition of motion in video by adapting the knowledge in the image. By exploring the common components of tagged videos and images, the adapted knowledge is used to learn relevant action semantics. However, most existing video action recognition methods have the problem of lacking sufficient labeled training videos [3].

C. MAIN CONTENT

(1) This article mainly uses zairinxfpga's Spartan6 as the core chip, collects the digital image information output by the camera through the camera link interface, and transmits it to the camera system high-speed NAND flash memory image for temporary DDR2 SDRAM memory and high-speed image storage table. Then delete the digital image information stored in the system and download it to the computer through the USB3.0 interface. Based on the detailed introduction of the technology of each system unit, the circuit design of each high-speed unit and the logic method of speed matching between each unit are mainly introduced. The system can quickly and accurately collect and store image data.

(2) The main content of this article is the action recognition research based on human common information, background information and color information. From the perspective of expressing personal movements, the information provided by the joint points is considered to be an improvement of the depth information of the human body. Therefore, if the information of the human joint points can be accurately obtained from the background information, the information of the pronunciation points can be replaced by the background information To express human attitudes. Then confirm the human movement. However, when a person's movement is related to an object in his hand, information through the joint points alone is not enough. Therefore, in this document, for the held object, the connection point, depth and color information are used to take a color image of the object, identify the type of target, and perform motion recognition in conjunction with the traffic characteristics based on the connection point information.

II. ACTION RECOGNITION METHOD

A. DATA ACQUISITION OF ACTION RECOGNITION SIGNAL SOURCE

The signal acquisition module uses HTC HD2 mobile phone with Android 2.3.3 system equipped with Qualcomm Adren200 microprocessor,

Its main frequency is 1GHz, 256MB of read-only memory and 224M of memory, and comes with a Wifi connection. The computer host includes 3 MEMS sensors, 3-axis geomagnetic sensors and 3-axis acceleration sensors, and can transfer data to obtain these three sensors according to the system API [4].

The collected human inherent motion signal data must have a specific position offset. Here the signal source is pre-processed, its role is to eliminate excess noise, to prevent interference and degradation of important signals and data, the cause of degradation is caused by circuit impedance matching. The preprocessing usually consists of filters and normalization.

1) FILTER

Filters can be divided into the following four according to different feasible signal frequencies, which are high-pass, low-pass, band-pass, and band-repair filters, and can also be divided according to the response width of the filter: finite pulse and wireless pulse filter[5].

2) NORMALIZATION

Normalization is used to process the data. Its function is to distribute the samples uniformly. The general methods used are as follows:

1) Among them, the most representative method is linear function conversion, the formula is expressed as:

$$y = \frac{x - MinV}{MaxV - MinV} \tag{1}$$

2) Followed by the logarithmic function conversion, the formula is shown in (2):

$$y = \log_{10} x \tag{2}$$

3) The most commonly used thing is the arc tangent function conversion, the formula can be written:

$$y = \frac{\arctan(x) * 2}{\pi} \tag{3}$$

The value before conversion of the function is x, and the value after conversion is y, and the maximum value of the sample data is represented by MaxV, and the minimum value of the sample data is MinV [6].

In pattern recognition, because the sample data is too long and the data dimension is too high, the sample data cannot be directly input into the classifier for action classification. Therefore, a feature space is constructed by a feature generation association algorithm. In order to classify and recognize actions, it is necessary to input finite-dimensional features in the classifier.

There are many ways to create functional space, which can be divided into time domain and frequency domain. The general functions of time domain include absolute average, distortion, acidity, AR model parameters, and intermediate frequency. The development of science has become more practical and new functions have been discovered. For example, advanced statistical techniques have been widely used in various fields. The commonly used secondary statistics are commonly used signal analysis functions. They are the same in time and frequency, and are very sensitive to external noise. Higher-order statistics can avoid these shortcomings. The concept of higher-order statistics was advocated in the 1960s, and its value was first discovered in the field of modern signal processing, and it has gradually become a key method of signal processing [7].

This work is licensed under a Creative Commons Attribution 4.0 License. For more information, see https://creativecommons.org/licenses/by/4.0/.

This article has been accepted for publication in a future issue of this journal, but has not been fully edited. Content may change prior to final publication. Citation information: DOI 10.1109/ACCESS.2020.3020892, IEEE Access

During the movement of the human body, if the posture of the human body changes, the coordinate system of various instantaneous sensors will change. In order to reduce the calculation complexity and eliminate the coordinate mapping relationship between the acceleration output values at different times, the amplitude of the acceleration is defined here, which is denoted as BB(t).

$$BB(t) = \sqrt{a_{x,t}^2 + a_{y,t}^2 + a_{z,t}^2} \tag{4}$$

Principal component analysis (PCA) is a method commonly used to simplify the original multivariate data set and reduce the number of variables. The linear mapping is realized, and the data is displayed on different axes of the new coordinate system, so the transformed characteristic carriers are perpendicular to each other. In the main analysis based on the dispersion-based component, the transformed carrier and the original carrier are used. According to the value of distribution contribution, the transformed features are classified and divided into the first main element, the second main element, etc[8]. Principal component analysis is often used to reduce the dimension of the data set. By calculating the dispersion contribution value, only this secondary feature subset can be used to maintain the few secondary features that contain most of the information in the original feature space. Not the entire feature space, but the size of the feature is reduced [9].

B. SIGNAL DATA CLASSIFICATION AND RECOGNITION (KNN) ALGORITHM

The signal classification and recognition algorithm is based on the shortest distance principle of classification and recognition. Its advantages are intuitive and simple. Want to achieve the classification effect of Bays decision can be completed by theoretically complete prior knowledge. It can be said to be the most complex and important identification technology for distribution [10].

Suppose the data set: $\{y_i^{(i)}\}, i = 1,2,...,c,..., j = 1,2,..., N_i$, the number of samples of w_i is the i-th category of N_i . Among them, the main classification idea can be expressed as: test the distance between the unknown number x to be tested and the sample $y_i^{(i)}$, and then use it as the closest class to the sample. According to this classification idea, the decision function can be obtained as:

$$d_i(x) = \min_{j=1,2,...,N_i} \| x - y_j^{(i)} \|, i = 1,2,...,c \tag{5}$$

The decision rules are:

$$m = \arg\min_{i=1,2,...,c}(d_i(x)), x \in w_m \tag{6}$$

The above method is often referred to as the nearest neighbor method or the 1-nearest neighbor method, because only the sample type closest to the known pattern is determined. The nearest sample selected K test data, the purpose of which is to eliminate general contingency and improve reliability. The type of the k nearest neighbors with the most samples, to which category x is assigned. The probability of erroneous determination of the KNN algorithm is directly related to the measurement of a specific distance when the number of samples is limited. Therefore, using the appropriate distance function, selecting the closest sample according to this will increase the classification accuracy. This algorithm is suitable for class domain classification with large sample size [11].

The modified KNN method is used here. Find the k point closest to the test vector in each type of training set, and take the average of the k distance of each type to indicate the distance between the test vector and the class. The test vectors are classified into the class with the smallest average distance. The nearest neighbor classifier is a direct inference method widely used in the field of pattern recognition. The special function of designing samples using KNN is that there is no need to build a model because it is simple and intuitive and can be easily understood, but it requires us to maintain historical data and calculate the cost of the entire operation process. There is no data distribution information for distance measurement, so Euclidean distance is usually used in practical applications [12].

C. GAUSSIAN MIXTURE MODEL (GMM) ALGORITHM

The Gaussian mixture model (GMM) has achieved excellent results in the fields of numerical approximation, speech recognition, human feature recognition, image classification, image noise removal, target tracking and recognition. In the literature, the Gaussian mixture model is used for background modeling. As a result, the detection scanning area is reduced and the detection speed is increased. The mixed Gaussian model has the following definitions:

$$p(x) = \sum_{z=1}^{Z} \pi_z p(x \mid \lambda_z) \tag{7}$$

Among them:

$$p(x \mid \lambda_z) = N(x \mid u_z, v_z) \tag{8}$$

In estimating parameters, the most-likelihood method is often used. Since the result of multiplying multiple probability values is very small, the floating point of the computer is easy to underflow. The usual method is to take probability and logarithm, the likelihood function is as follows:

$$L(X \mid \pi_1, u_1, v_1, ..., \pi_2, u_2, v_2) = \sum_{i=1}^{N} \log p(x_i) \tag{9}$$

The EM algorithm solves the GMM parameters as follows:

$$u_z = \frac{1}{N} \sum_{i=1}^{N} w_i(z) x_i \tag{10}$$

$$v_z = \frac{1}{N_Z} w_i(z)(x_i - u_z)(x_i - u_z)^T \tag{11}$$

$$N_z = \sum_{i=1}^{N} w_i(z) \tag{12}$$

$$\pi_z = \frac{N_Z}{N} \tag{13}$$

III. IMAGE ACQUISITION SYSTEM EXPERIMENT

A. AEROBICS TRAINING ACTION RECOGNITION DATA SET

MSRC-12 (Microsoft Research Cambridge-12) human motion data set is a sequence of motions of human joint point data collected through a proprietary device. Each frame of the

This work is licensed under a Creative Commons Attribution 4.0 License. For more information, see https://creativecommons.org/licenses/by/4.0/.

This article has been accepted for publication in a future issue of this journal, but has not been fully edited. Content may change prior to final publication. Citation information: DOI 10.1109/ACCESS.2020.3020892, IEEE Access

motion contains 20 joint points of the human body. At 30 Hz, the accuracy of joint point recognition is 2 cm. The data set contains 594 action sequences, a total of 719,359 frames, human posture and joint data, a total of 6,144 actions, obtained by 12 actions performed by 30 people [13].

The data set is provided in the form of a 594 CSV file and the corresponding 594 activity data set, with Matlab code, used to verify the integration of the data set and the visualization of human bones. The content of action sequence data is saved in the CSV file [14]. Each CSV file contains 8 to 12 action examples. In a specific instruction method, the same type of action is performed by the same person. The tag stream file marks the frame number where the action instance ends.

In the experiment, as the research database, the aerobic exercise decomposition database and the single aerobic exercise decomposition database were selected and recorded as database A and database B in sequence. Database A has 120 aerobics videos, and the video has 10 aerobics exercises, which are implemented in turn by 12 aerobics athletes. The data set was shot in the actual environment containing lighting information and was partially blocked. Database B contains 15 sports bodybuilders, a total of 65 videos. The video resolution of the two databases is 720 pixels × 480 pixels, and the rate is 80 frames per second [15].

B. IMAGE ACQUISITION SYSTEM CONSTRUCTION

High-speed graphics acquisition systems are usually completed using a high-speed interface and memory. The data input to the camera connection interface is associated with the FPGA. The FPGA can store data and output data. Of course, the most important thing is to display the data through the display. The specific structure is shown in Figure 1:

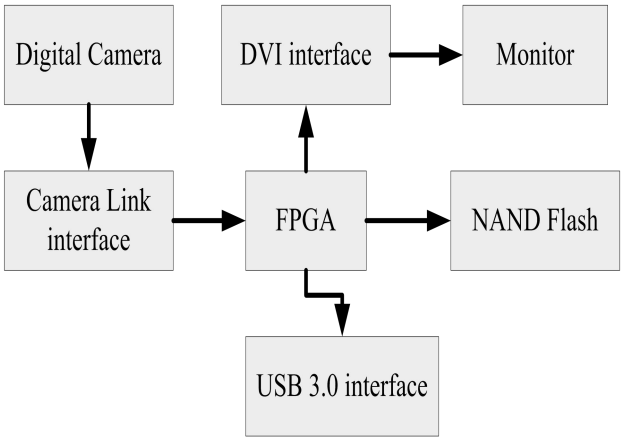

FIGURE 1. Structure diagram of image acquisition system

As the control core of the system, FPGA connects all the modules and controls the image data of all steps [16].

The function of the input and output data structure is to receive image signals and video from a digital camera and send it to the FPGA for later use. This is a very popular high-speed camera interface with only one acquisition interface. The LVDS signal from the camera converts it to the TTL signal used in the system and sends it to the FPGA [17].

The display module is used to observe the image collected during the acquisition process or reproduce the image information stored in the storage chip after the acquisition, and is only available when the DVI interface is connected to the screen.

The storage unit is the core of the high-speed image acquisition system. The collected image data is retrieved by the FPGA and stored in the system through the latent memory. DDR2 SDRAM is used to store the data and finally stored in the NAND memory [18]. The stored data will eventually be uploaded to the computer for processing or storage. The data output connector will also be used for this purpose. The USB 2.0 interface is used to connect to the computer. The USB interface is the most commonly used interface on the computer. The new version of USB 2.0 also significantly improves performance in all aspects.

VI. RECOGNITION AND ANALYSIS OF AEROBICS TRAINING ACTIONS

A. ANALYSIS OF ACTION INSTANCE RECOGNITION RESULTS

The purpose of this article is to test the effect of the action segmentation model in identifying action sequences. In order to compare the recognition results of action sequences, we first need to obtain the recognition rate of a single action instance. In this paper, we will refer to the experimental results of Chapter 3 on the recognition of action instances [19]. After identifying the action sequence, the function parameters of the action code graph are set to M=2, N=30, P=8, and the similarity r of the PCA dimension reduction is set to 0.94. This parameter setting may not be suitable for the recognition rate of the action data set MSS, but because the same experimental conditions are set, it will not affect the purpose of the comparative experiment [20]. In this experiment, motion recognition is performed based on the flow of a single motion instance of the joint point of the bone in Chapter 3. In order to make the table simple and tidy, the seven actions of the action example data set MTS-J (handshake, hug, greeting, refusal, take a glass of water, send the stapler, send the drink) are denoted by A1 ~ A7. In this experiment, the test uses K-segment cross-validation. In the action instance data set MIS-J made on this white paper, there are only 25 action instances of each type, so the K value is 3. In the experiment, based on the characteristics of the action coding table shown in Table 1, the recognition rates of seven types of action examples were obtained. The data in Table 1 is displayed in the form of a percentage system [21].

TABLE I
SINGLE ACTION INSTANCE RECOGNITION CONFUSION MATRIX

	B1	B2	B3	B4	B5	B6	B7
B1	31	0	5	22	0	0	22
B2	0	97	0	35	22	2	0
B3	0	40	20	14	45	34	0
B4	6	0	0	0	33	0	0
B5	0	0	4	21	0	66	0
B6	14	12	2	11	2	3	34
B7	23	0	0	0	33	4	44

This work is licensed under a Creative Commons Attribution 4.0 License. For more information, see https://creativecommons.org/licenses/by/4.0/.

This article has been accepted for publication in a future issue of this journal, but has not been fully edited. Content may change prior to final publication. Citation information: DOI 10.1109/ACCESS.2020.3020892, IEEE Access

Calculate the main diagonal of Table 1 so that the average recognition rate of the action sequence is 63.5%. As can be seen from the data in the table, the proportion of action A1 is erroneously identified as B6 (conveying stapler) and B7 (conveying beverage). This is because the average recognition rate of the three actions is only 37.8% [22]. These three actions are similar to the human skeleton coordinate space. Even if they only rely on skeleton information, they cannot fully distinguish these three types of actions. In other actions, the recognition rate of the action code based on the junction information of this article may decrease the recognition rate and stabilize at around 88% [23].

B. ANALYSIS OF ACTION SEGMENTATION MODEL RESULTS

Split all the static units of the action sequence data set MSS-J, and add the "inter-action static unit" and "action internal fixed unit" to the divided static unit according to the starting frame number of the single action instance marked in the action sequence s Mark". Calculate the number of columns in all static units and create a static unit column number data set SUWS. Each sample of the data set includes: a one-dimensional scalar label of "stationary unit between actions" and "stationary unit within actions" [24]. From the two samples of the static unit time length data set SUWS, the interaction unit and the internal action unit randomly select 2/3 of the corresponding sample number to form a training set, and the remaining samples are the test group [25].

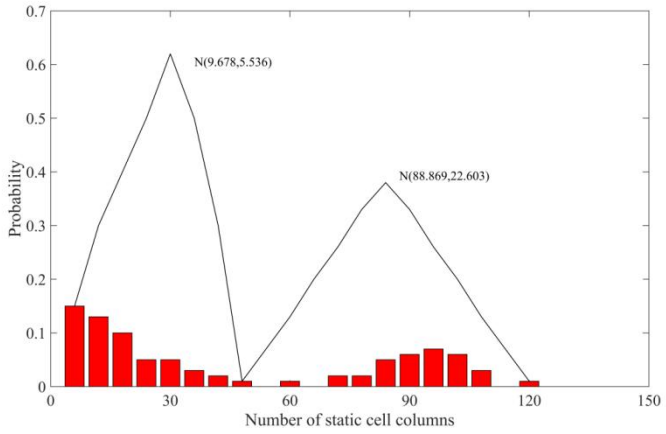

FIGURE 2. Probability distribution of stationary units in the training set

During training, the above method is used to train a mixed Gaussian model using the training set to obtain the Gaussian distribution of the static unit between the actions and the static unit within the actions, respectively N (9.678, 5.536) and N (88.869, 22.603), the weight of the two Gaussian distributions The values are 0.6168 and 0.3832, respectively. Draw two Gaussian distribution curves as shown in Figure 2. The abscissa of the intersection of the two Gaussian distribution curves in the figure is 50, which means that the Gaussian mixture model after training will use 50 as the threshold to determine the static unit category [26].

TABLE II
RECOGNITION RATE ON RANDOM TEST SET

i times	1	2	3	4	5	average value
Action unit	13	15	17	14	16	15
Stationary unit	23	26	21	29	26	25
Recognition rate	96.34	96.42	96.26	95.35	97.33	96.34

The trained mixed Gaussian model is used to predict the static unit category on the test set. In order to make the experimental results persuasive, this paper conducts a random selection of the training set on the data set SUWS for 5 tests to obtain the results shown in Table 2. The size of the training set randomly collected for these 5 times remains unchanged, which is still 2/3 of the original data set [27].

C. ANALYSIS OF AEROBICS TRAINING MOVEMENT RECOGNITION

In order to facilitate the analysis, first conduct an experimental test against database B. Choose a group of aerobics decomposition actions in database B arbitrarily, and recognize them by action recognition method, dictionary learning method and hierarchical time memory method. The results are shown in Figure 3.

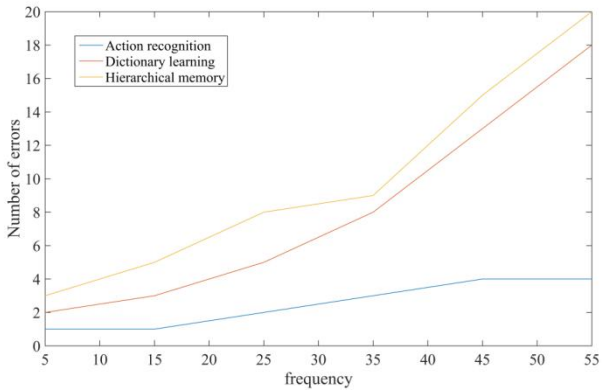

FIGURE 3. Comparison of three methods of recognition results

As can be seen from the analysis in Figure 3, the behavior recognition method is to identify the aerobic exercise decomposition motion images with the fewest errors and the most accurate results, and can effectively identify various aerobic exercise decomposition behaviors, and dictionary learning methods and graded time storage The recognition result of the method is wrong, indicating that the method of the paper has a high recognition accuracy [28].

According to the data analysis of Figure 3, in the recognition results of aerobic exercise decomposition exercise, the method of this paper is the most confusing. The dictionary learning method confuses the cross exercise of the chest with the chewing exercise, stepping exercise, stepping exercise, and stepping exercise. In the hierarchical time memory method, the chest crossover motion is confused with the bite motion,

This work is licensed under a Creative Commons Attribution 4.0 License. For more information, see https://creativecommons.org/licenses/by/4.0/.

This article has been accepted for publication in a future issue of this journal, but has not been fully edited. Content may change prior to final publication. Citation information: DOI 10.1109/ACCESS.2020.3020892, IEEE Access

stepping motion, and stepping motion. The other two methods are based on the recognition confusion matrix of database B, and the degree of confusion is higher than the method in this paper.

In order to further verify the effectiveness of the thesis method, this paper uses the method, dictionary learning method and hierarchical time storage method to determine the aerobic exercise decomposition action in the database A. Figure 4 shows the comparison results of the recognition accuracy of the three methods in different scenarios.

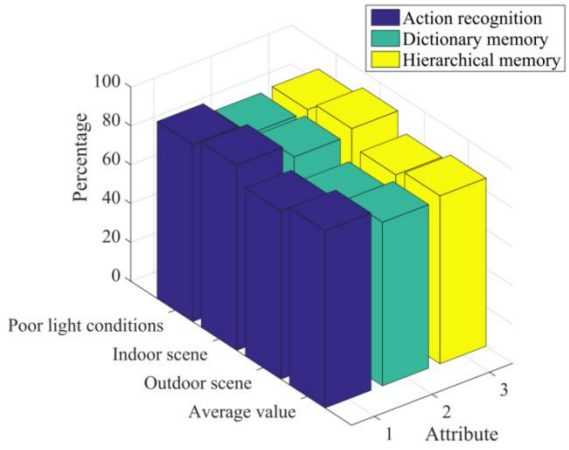

FIGURE 4. Comparison of three methods for recognition accuracy

Analysis of FIG. 4 shows that in the database B, the three methods have relatively low recognition accuracy in scenes with severe lighting conditions and outdoor scenes, and relatively high recognition accuracy in indoor scenes. Since the recognition accuracy of different scenes is very high, we will further verify the accuracy of this action recognition method [29].

D. ANALYSIS OF IMAGE ACQUISITION SYSTEM

(1) IMAGE ACQUISITION MODULE

The OV9650 CMOS image sensor is used to complete the collection of graphic data. The OV9650 workflow uses the IIC control bus to initialize registers to form a CAMIF work unit. Data is sent through the SCCB interface. After the initialization is complete, the image collection driver will be loaded into the kernel to execute the camera application. The software viewer.exe executes the IP address http://192.168.1.125, sets the port number to 8080, and displays the collected image data. The image resolution is 640*480, the image is saved in the directory specified by the Linux system, the path is /txcj/xiaoweb.

(2) WIRELESS TRANSMISSION MODULE

The system implements communication between wireless networks and remote devices. Port the Wifi driver to the development board, start the development board to complete the relevant configuration data, form the wireless network card IP, form the default gateway, display the current connection status, and test the connection data. After ping, the received packet information will be displayed, proving that the Wifi connection is successful and can work normally.

(3) BOA SERVER MODULE

The system realizes the transplantation of Boa server. After executing the Boa server, users only need to enter the IP address in the browser to access the Boa server. The server can also provide support for static web pages and CGI programs, so the application is very flexible. Using the HTML language can enable the Boa server to interact with the browser. To display the captured image information, enter the address on the web page.

The system consists of an image acquisition module, a wireless transmission module, and a Boa server module. The three modules are combined to form an embedded image acquisition system. Equipped with a wireless transmission function, it reduces the chance of transmitting data through complex lines, realizes Wifi wireless transmission, and expands the application range.

The image acquisition system outputs image data after being powered on normally. The CamExpert control software will detect the Camera Link synchronous clock signal and line valid and frame valid signals for the first time, after which data can be displayed and stored. The JTAG signal and data stream output from the FPGA chip complete the configuration of the CMOS image sensor, and the CMOS image sensor works normally to output image data. The image data output by the CMOS image sensor is divided into two types: reset data and image data. From the output image, it can be seen that there is an inconsistent response between the image data output by different arrays. Simultaneous output of reset data and image data makes the data output The channel utilization rate is low, especially when the CMOS image sensor has a high clock frequency. If the generated high-speed data stream contains both the reset signal and the image data, it is difficult to output all the data at the same time using the Camera Link interface. For the purpose of improving the effective utilization rate of data output resources, an image data processing function module is added to the FPGA software to appropriately process the image data and reset data, thereby reducing the redundant information of the transmitted data and improving the efficiency of data transmission [30]. The reset data is combined with the image output on the image data board. The data synthesis effectively reduces the channel bandwidth requirements for data transmission. The use of a lower frequency synchronous clock can still successfully complete the data transmission of the CMOS image acquisition system. The lower clock The frequency has the power consumption to control the Camera Link encoding chip and related control logic. Through the analysis of the image sensor, it can be concluded that the effective pixel resolution of the image sensor is $1240*2350$, and the actual output image resolution is $2590*2350$. This is because the CIS2521 image sensor has 18 rows of dark pixels at the top and bottom (including 9 rows of shading pixels and 9 rows of reset pixels), and there are 18 columns of dark pixels on the left and right (including 9 columns of shading pixels and 9 columns of reset pixels). At the same time, because the ADC resolution of the sCMOS image sensor is 14 bits, and Camera Link transmission uses 16-bit data to represent the output value of the image data of one pixel, the highest bit data is replaced with 16 by 16-bit data. -bit data, so the output image data cannot be seen in white when displayed by CamExpert.

V. CONCLUSIONS

This paper introduces a GMM-based segmentation algorithm, which needs to first obtain the coding graphics of the action

This work is licensed under a Creative Commons Attribution 4.0 License. For more information, see https://creativecommons.org/licenses/by/4.0/.

This article has been accepted for publication in a future issue of this journal, but has not been fully edited. Content may change prior to final publication. Citation information: DOI 10.1109/ACCESS.2020.3020892, IEEE Access

sequence, and define the static unit between actions according to the action coding diagram. Use the static unit between actions as the basis of segmentation to segment the sequence of actions. Through comparison experiments, the average recognition rate of the binding data set of action examples is 69.1%, and the average recognition rate of the binding data set of action sequences is 65.1%. For the realization of sequence segmentation, the recognition rate of information can be greatly reduced.

This paper studies the circuit design of the high-speed image acquisition system. Based on the analysis of the extensive application and research situation of the image acquisition system, a series of high-performance devices manufactured by the rapid development of electronic technology are designed as a board-based design, NAND flash memory high-speed image acquisition system. First of all, the system can only obtain Camera Link images in the basic mode. In order to expand the design of the system later, the circuit principle of the higher-speed operation mode is being explored.

In this paper, a data acquisition system is designed based on the typical human inherent motion recognition, and the realization effect is displayed in the front-end system. It describes the action recognition function that people already have. Its process starts with the acquisition of information data, followed by data preprocessing, and finally action classification. As an important part of the system, the mobile front-end based on data collection of wireless sensor network system has designed the main function of motion recognition. In addition, the data collection method and characteristic values of the human falling motion signal data are also introduced On the basis of calculation, the process of motion recognition algorithm is realized, and a complete experiment is designed. Finally, the statistics of the data are analyzed and summarized.

REFERENCES

[1] Ye W. "Teaching Effectiveness Evaluation of Physical Education and Aerobics Training Based on Data Mining Method," *Revista be La Facultad be Ingenieria*, vol. 32, no. 2, pp. 727-733, 2017.
[2] Gupta P S., Choi G S. "Image Acquisition System Using on Sensor Compressed Sampling Technique," *Journal of Electronic Imaging*, vol. 27, no. 1, pp. 367-382, 2018.
[3] Zhang J., Han Y., Tang J. "Semi-Supervised Image-to-Video Adaptation for Video Action Recognition," *Cybernetics IEEE Transactions on*, vol. 47, no. 4, pp. 960-973, 2017.
[4] Zhang H. "Hadoop Education Platform Application for Aerobics Teacher Training: a Big Data Analysis," *Boletin Tecnico/Technical Bulletin*, vol. 55, no. 6, pp. 145-153, 2017.
[5] Qu H. "Application of Kinect Technology in Blind Aerobics Learning," *International Journal of Emerging Technologies in Learning*, vol. 12, no. 12, pp. 103, 2017.
[6] Podstawski R., Markowski P., Choszcz D. "Effectiveness of Martial Arts Training Vs. Other Types of Physical Activity: Differences in Body Height, Body Mass, Bmi and Motor Abilities," *South African Journal for Research in Sport, Physical Education and Recreation*, no. 3911, pp. 111-133, 2017.
[7] Qin W Y. "Design and Implementation of Image Acquisition System based on Stm32," *International English Education Research: English Version,* vol. 000, no. 002, pp. 64-66, 2017.
[8] Behrens M., Müller, Karoline, Kilb J I. "Modified Step Aerobics Training and Neuromuscular Function in Osteoporotic Patients: a Randomized Controlled Pilot Study," *Archives of Orthopaedic & Trauma Surgery*, vol. 137, no. 2, pp. 195-207, 2017.
[9] Lee Y H., Khalil-Hani M., Bakhteri R. "A Real-Time Near Infrared Image Acquisition System based on Image Quality Assessment," *Journal of Real Time Image Processing*, vol. 13, no. 1, pp. 103-120, 2017.
[10] Chen S., Guo Z., Feng J. "An Improved Contact-Based High-Resolution Palmprint Image Acquisition System," *IEEE Transactions on Instrumentation and Measurement*, pp. 99, 1-1, 2020.
[11] Hu J., Xie L., Zou W. "Design of Miniature Image Acquisition System Based on Low Power System on Chip," *Hunan Daxue Xuebao/Journal of Hunan University Natural ences*, vol. 46, no. 2, pp. 86-91, 2019.
[12] Wang W., Cai L. "On the Developmentof an Effective Image Acquisition System for Diamond Quality Grading," *Applied Optics*, vol. 57, no. 33, pp. 9887, 2018.
[13] Liu Yuanyuan., Zhang Yuehai., Yu Guiying. "High Resolution Image Acquisition System for Rice Pest," *Laser & Optoelectronics Progress*, vol. 55, no. 2, pp. 021006, 2018.
[14] Zuzda J G., Latosiewicz R., Bras R. "Application of Thermal Imaging and PWC170 Test for the Evaluation of the Effects of a 30-Week Step Aerobics Training," *Nephron Clinical Practice*, vol. 51, no. 1, pp. 85-99, 2017.
[15] Li L., Dai S. "Action Recognition With Spatio-Temporal Augmented Descriptor And Fusion Method," *Multimedia Tools and Applications*, vol. 76, no. 12, pp. 13953-13969, 2017.
[16] Wang H., Wang L. "Cross-Agent Action Recognition," *IEEE Transactions on Circuits and Systems for Video Technology*, vol. 28, no. 10, pp. 2908-2919, 2018.
[17] Shao Z., Li Y., Zhang H. "Learning Representations from Skeletal Self-Similarities for Cross-view Action Recognition," *IEEE Transactions on Circuits and Systems for Video Technology*, pp. 99, 1-1, 2020.
[18] Jiang X., Xu K., Sun T. "Action Recognition Scheme based on Skeleton Representation with DS-LSTM Network," *IEEE Transactions on Circuits and Systems for Video Technology*, pp. 99, 1-1, 2019.
[19] Liu Y., Lu Z., Li J. "Hierarchically Learned View-Invariant Representations for Cross-View Action Recognition," *IEEE Transactions on Circuits and Systems for Video Technology*, vol. 29, no. 8, pp. 2416-2430, 2019.
[20] Zhao S., Liu Y., Han Y. "Pooling the Convolutional Layers in Deep ConvNets for Video Action Recognition," *IEEE Transactions on Circuits and Systems for Video Technology*, vol. 28, no. 8, pp. 1839-1849.
[21] Chen Y., Cai M., Zhou X. "A Robust Spatial Information-Theoretic GMM Algorithm for Bias Field Estimation and Brain MRI Segmentation," *IEEE Access*, pp. 99, 1-1, 2020.
[22] Wang Z., He D., Li B. "Clustering of Copper Flotation Process Based on the AP-GMM Algorithm," *IEEE Access*, pp. 99, 1-1, 2019.
[23] Chen H., Cui Y., Li S. "An Improved GMM-Based Algorithm With Optimal Multi-Color Subspaces for Color Difference Classification of Solar Cells," *IEEE Transactions on Semiconductor Manufacturing*, vol. 31, no. 4, pp. 503-513, 2018.
[24] Aminikhanghahi S., Shin S., Wang W. "A New Fuzzy Gaussian Mixture Model (Fgmm) based Algorithm for Mammography Tumor Image Classification," *Multimedia Tools and Applications*, vol. 76, no. 7, pp. 10191-10205, 2017.
[25] A T K V., A M K H., B H L L. "An Em Algorithm for Gmm Parameter Estimation in the Presence of Censored and Dropped Data With Potential Application for Indoor Positioning," *ICT Express*, vol. 5, no. 2, pp. 120-123, 2019.
[26] Ma B., Xu M., Wu Z. "A Fpga Implementation of Gmm Mud Algorithm for Space Formation Aircraft Communication System," *MATEC Web of Conferences*, vol. 309, no. 1, pp. 01004, 2020, .
[27] Navneet S., Ghedia, C H., Vithalani., Ashish Kothari. "Performance Evaluation of Crowd Analysis Algorithm using Modified GMM and Adaptive Thresholding," *Indian Journal of Science & Technology*, vol. 10, no. 17, pp. 1-7,2017.
[28] Wu Xiaojun., Huang Chaohui. "Application and Research Status of ZigBee Wireless Data Transmission Technology in Welding Parameter Collection and Analysis," *Electric Welding Machine*, vol. 048, no. 004, pp. 99-103, 2018.
[29] Wu Yuanfu., sun Mengyun., Lei Yu. "Research on Application of Wireless Power Transmission Technology in Groundwater," *Automation and Instrumentation*, vol. 000, no. 012, pp. 195-197, 201, 2018.
[30] Liang Zhanze. "Application of Wifi Wireless Technology in Data Transmission of Shearer," *Shaanxi Coa*l, vol. 36, no. 005, pp. 105-107, 2017.

This work is licensed under a Creative Commons Attribution 4.0 License. For more information, see https://creativecommons.org/licenses/by/4.0/.

This article has been accepted for publication in a future issue of this journal, but has not been fully edited. Content may change prior to final publication. Citation information: DOI 10.1109/ACCESS.2020.3020892, IEEE Access

Haiying Guo, an associate professor was born in Yingxian County, Shanxi Province,P.R. China, in 1978. She received the master's degree in Education from Shanxi University, China. Now, she is studying for her Ph.D. atKyungsung University in South Korea.Her main research direction is Sports Humanities and Sociology.
E-mail: ghy_791204@126.com.

Hui Liu, an associate professor, was born in Yuci, Shanxi, P.R. China, in 1978.He received his master's degree in Education from Shanxi University, China. His main research direction is Sports Humanities and Sociology.
E-mail: lh_780722@126.com

Xiaoming Liu was born in Qinhuangdao, Hebei Province, China in 1979. Research direction: sports human body science, folk sports, etc.
E-mail: xliu7879@163.com.

This work is licensed under a Creative Commons Attribution 4.0 License. For more information, see https://creativecommons.org/licenses/by/4.0/.